

Generation of functional thymic organoids from human pluripotent stem cells

Stephan A. Ramos,¹ Lucas H. Armitage,¹ John J. Morton,² Nathaniel Alzofon,² Diana Handler,⁷ Geoffrey Kelly,⁷ Dirk Homann,³ Antonio Jimeno,^{2,4} and Holger A. Russ^{1,4,5,6,*}¹Barbara Davis Center for Diabetes, University of Colorado Anschutz Medical Campus, Aurora, CO 80045, USA²Division of Medical Oncology, Department of Medicine, University of Colorado School of Medicine, Aurora, CO 80045, USA³Diabetes, Metabolism and Obesity Institute, Icahn School of Medicine at Mount Sinai, New York, NY 10029, USA⁴Charles C. Gates Center for Regenerative Medicine, University of Colorado School of Medicine, Aurora, CO 80045, USA⁵Diabetes Institute, University of Florida, Gainesville, FL 32610, USA⁶Department of Pathology and Therapeutics, University of Florida, Gainesville, FL 32610, USA⁷Human Immune Monitoring Center, Icahn School of Medicine at Mount Sinai, New York, NY 10029, USA*Correspondence: holger.russ@ufl.edu<https://doi.org/10.1016/j.stemcr.2023.02.013>

SUMMARY

The thymus is critical for the establishment of a functional and self-tolerant adaptive immune system but involutes with age, resulting in reduced naive T cell output. Generation of a functional human thymus from human pluripotent stem cells (hPSCs) is an attractive regenerative strategy. Direct differentiation of thymic epithelial progenitors (TEPs) from hPSCs has been demonstrated *in vitro*, but functional thymic epithelial cells (TECs) only form months after transplantation of TEPs *in vivo*. We show the generation of TECs *in vitro* in isogenic stem cell-derived thymic organoids (sTOs) consisting of TEPs, hematopoietic progenitor cells, and mesenchymal cells, differentiated from the same hPSC line. sTOs support T cell development, express key markers of negative selection, including the autoimmune regulator (AIRE) protein, and facilitate regulatory T cell development. sTOs provide the basis for functional patient-specific thymic organoid models, allowing for the study of human thymus function, T cell development, and transplant immunity.

INTRODUCTION

The thymus is required for the development of a functional adaptive immune system, facilitating the generation of self-tolerant T cells that can respond to foreign antigens. Thymic epithelial cells (TECs) are divided into cortical and medullary (c/m) TECs, based on their location and function, and can be identified by the expression of KRTs 8 and 5, respectively. c- and mTECs originate from common bipotent progenitors, which first express KRT8 only and then co-express both keratins prior to bifurcating into c- and mTEC lineages (Kadouri et al., 2020). Age-related involution of the thymus results in decreased thymic function and naive T cell output and increased autoimmunity and disease risk (Coder et al., 2015; Palmer, 2013). Thymic dysfunction or absence can result from intrinsic and extrinsic factors, namely DiGeorge syndrome (DGS), *FOXP1* deficiency, infection, and/or radiation therapy (Duah et al., 2021; Kreins et al., 2021). Complete athymia is treated with hematopoietic stem cell or allogeneic thymus transplant; however, such treatments carry associated complications and depend on limited donor tissue (Janda et al., 2010; Kreins et al., 2021). Thus, an experimental model system to interrogate the mechanisms of thymic insufficiency and function is necessary and could serve to further the development of cell-based treatments for thymic defects.

Thymic organoids cultured at the air-liquid interface allow for the interrogation of thymic function and T cell development (Auerbach, 1960; Ceredig et al., 1989; Han

and Zúñiga-Pflücker, 2021; Mandel and Kennedy, 1978; Watanabe and Katsura, 1993; Watson et al., 1989). Functional human reaggregated thymic organoid cultures (RTOCs) made with expanded 1° TECs and thymic mesenchyme (TM) combined with allogeneic cord blood-derived hematopoietic stem cells (HSCs) support T cell development *in vitro* and *in vivo* (Chung et al., 2014). However, RTOCs depend on 1° tissue access, are allogeneic, and do not support negative selection.

TECs express Notch ligands, such as *DLL4*, which are critical for T cell commitment and differentiation. Indeed, transgenic OP9 or MS5 murine bone marrow stromal cells expressing human *DLL1* or *DLL4* support positive selection of developing murine and human T cells *in vitro* (Schmitt and Zuniga-Pflucker, 2002). Combining 1° HSCs (Seet et al., 2017) or human pluripotent stem cell (hPSC)-derived embryonic mesodermal progenitors (EMPs) (Montel-Hagen et al., 2019) with MS5-*DLL1/DLL4* cells, the Crooks group demonstrated T cell development in artificial thymic organoids (ATOs) *in vitro*. Though OP9-*DLL1* and ATO cultures eliminate the need for 1° tissue, the lack of thymic stromal cells and major histocompatibility complex (MHC) class II expression results in a skew toward CD8 T cell development. We sought to develop a thymic organoid model with isogenic hPSC-derived cell compartments that supports patient-specific TEC and T cell development *in vitro*.

Recently, we reported the directed differentiation of induced PSCs (iPSC) to functional thymic epithelial progenitors (TEPs) that support murine T cell development after



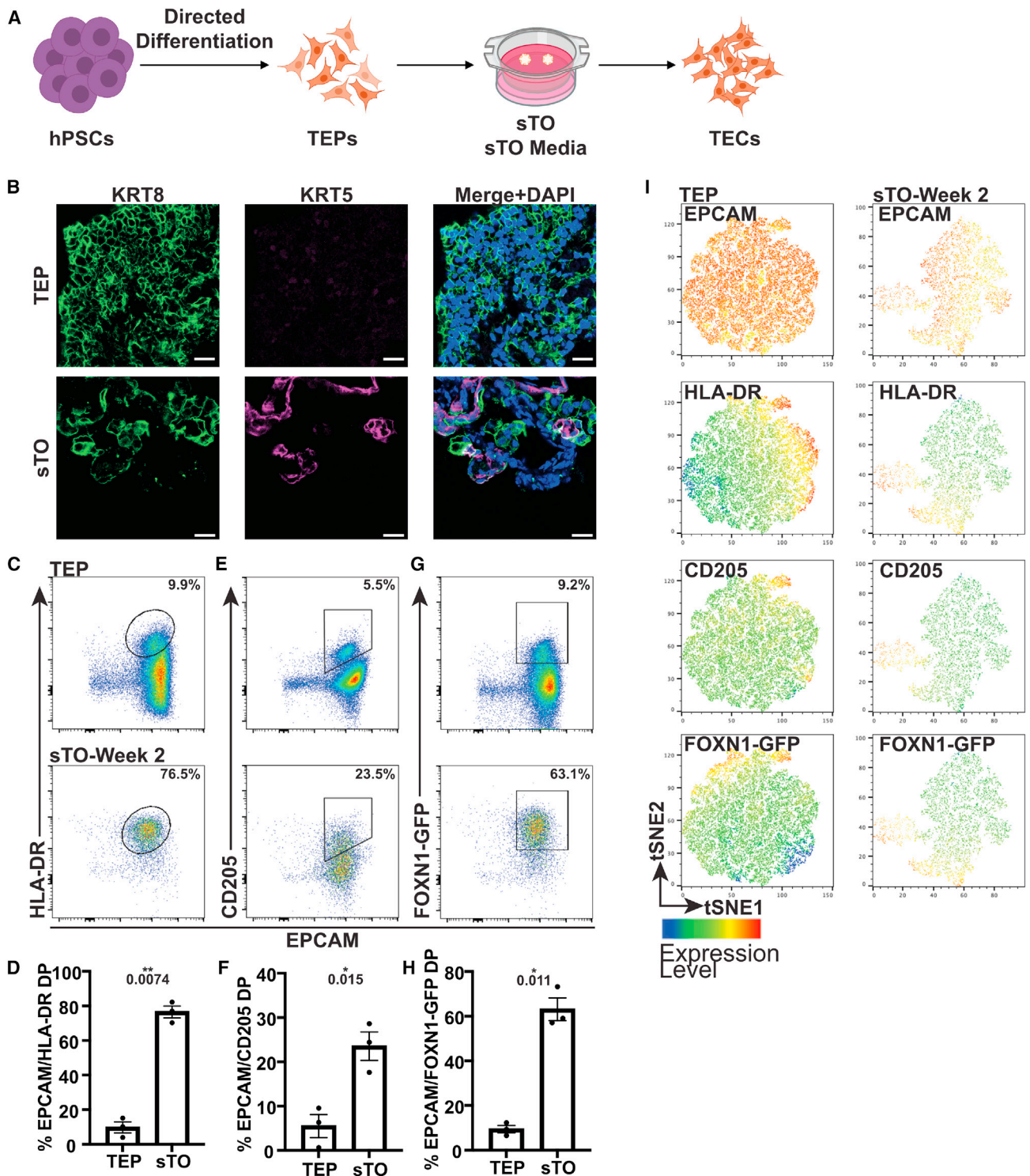


Figure 1. Generation of hPSC-derived TECs *in vitro*

(A) Schematic of TEP-only sTOs.

(B) Representative IF images of KRT8 (green) and KRT5 (magenta) in day 16–22 TEPs and week 2 TEP-only sTOs (TEPs, n = 2 independent experiment (ind. exp.), 2 hPSC lines; sTOs, n = 3 ind. exp., 2 hPSC lines).

(legend continued on next page)



transplantation in nude mice (Ramos et al., 2021). While differentiation of TEPs from human iPSCs has been demonstrated by multiple groups, *in vitro* generation of functional TECs has yet to be achieved (Chhatta et al., 2019; Parent et al., 2013; Soh et al., 2014; Volpi et al., 2017; Sun et al., 2013). We combined hPSC-derived TEPs, hematopoietic progenitor cells (HPCs), and mesenchymal cells to generate functional isogenic stem cell-derived thymic organoids (sTOs). sTOs support TEC development as demonstrated by HLA-DR, CD205, KRT5, and autoimmune regulator (AIRE) expression after 2–4 weeks *in vitro*, even in the absence of HPCs. AIRE, HLA-DR, and tissue-restricted antigen (TRA) expression suggests the potential for negative selection in this system. Importantly, sTOs support T cell development, including some regulatory T cells (Tregs). For the first time, to our knowledge, we demonstrate the generation of functional hPSC-derived TECs *in vitro*.

RESULTS

Activin A activation and BMP4 inhibition enhance *in vitro* TEP development

BMP4 and activin A regulate thymus development in both mice and humans (Lepletier et al., 2019; Ramos et al., 2021). To determine whether modulation of these pathways enhanced TEP generation, we differentiated 4 hPSC lines to TEPs and quantified the expression of TEP markers EPCAM and CD205 by flow cytometry (FC) analysis (Campinoti et al., 2020; Ramos et al., 2021) (Figures S1A–S1E). EPCAM expression increased in all new conditions (conditions 2–4), though not significantly (Figures S1A, S1C, and S1E). However, when compared directly with condition 1, activin A activation and BMP4 inhibition (condition 2) significantly increased the proportion of EPCAM⁺ and EPCAM⁺/CD205⁺ cells (Figures S1A–S1E). Thus, we employed this optimized TEP differentiation protocol for this study.

TECs develop in sTOs *in vitro*

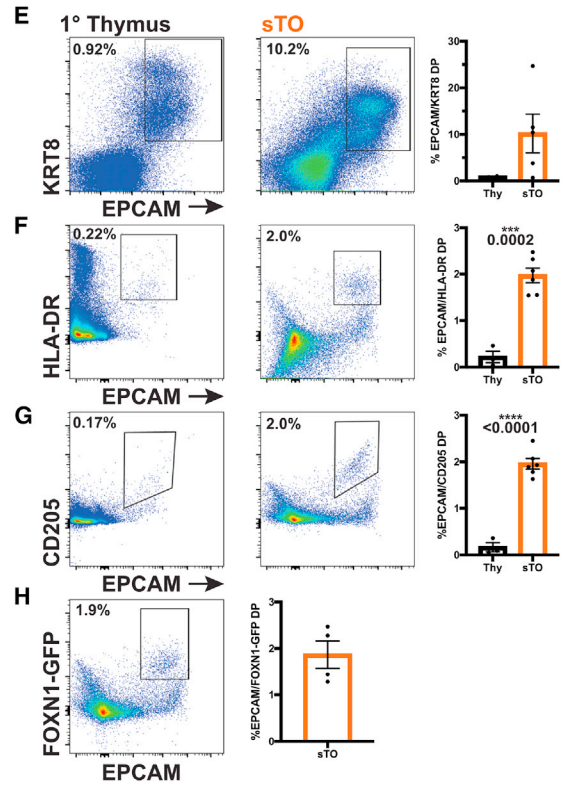
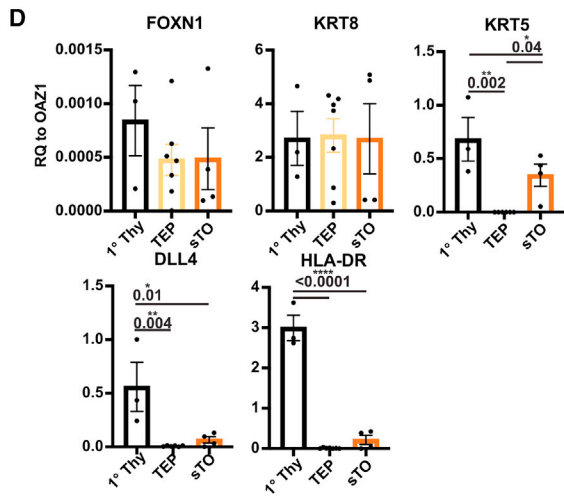
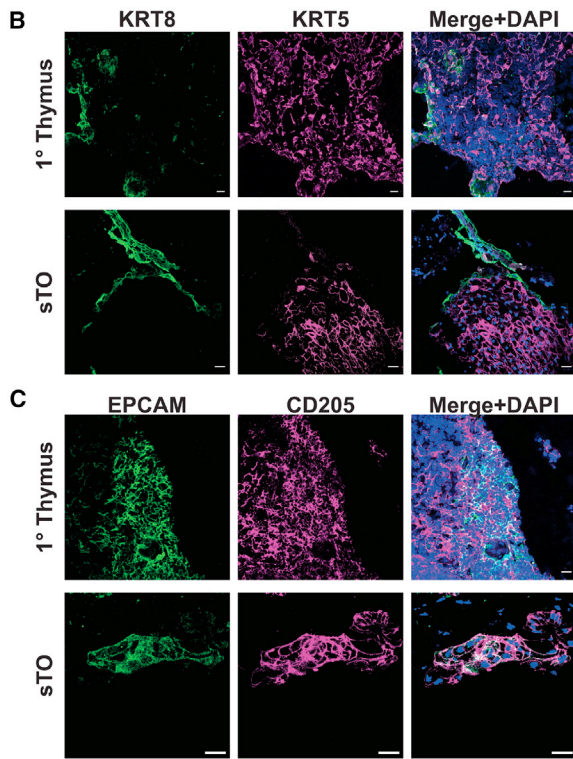
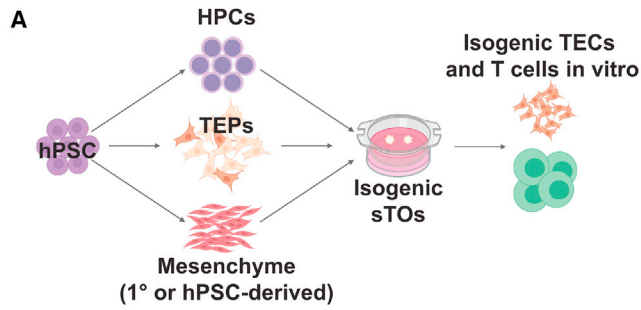
To test whether hPSC-derived TECs could be generated *in vitro*, we cultured differentiated day 16–30 TEP cultures at the air-liquid interface for up to 6 weeks in 3D and evaluated for TEC generation (Figure 1) (Chung et al., 2014). Early TEPs express KRT8 but lack KRT5 expression, however, after 2–3 weeks, TEP-only sTOs contain bipotent developing TECs that co-stain for KRT5/8 and KRT5⁺ mTEC-like cells (Figure 1B) (Parent et al., 2013; Ramos et al., 2021). We also observed a significant increase in HLA class II molecule

(HLA-DR) and CD205⁺ TECs compared with input TEPs (Figures 1C–1F). To quantify FOXP1 expression in the absence of a reliable antibody, we differentiated *FOXP1-GFP* reporter human embryonic stem cells (hESCs) to TEPs, generated TEP-only sTOs and quantified GFP expression by FC (Soh et al., 2014). Analysis of FOXP1-GFP expression showed ~64% EPCAM/GFP double positive (DP) cells in TEP-only sTOs compared with ~10% in 2D TEPs (Figures 1G and 1H). To visualize the expression of EPCAM, HLA-DR, CD205, and FOXP1 in relation to each other, we utilized t-stochastic neighbor embedding (tSNE) and observed expression of all markers within GFP⁺ clusters, indicating that sTO culture promotes TEP-to-TEC differentiation *in vitro*, even in the absence of HPCs (Figure 1I). To confirm that HPC-independent TEP-to-TEC development was not driven by the change from “TEP” to “sTO” media, 2D TEPs were cultured for 2 weeks in either medium. The proportion of EPCAM/HLA-DR, EPCAM/CD205, and EPCAM/GFP DP cells remained similar regardless of the media type, indicating that air-liquid sTO culture conditions are critical for further differentiation of hPSC-derived TEPs into TECs *in vitro*, not the associated media (Figures S1F and S1G).

TECs facilitate the education of thymocytes via positive and negative selection. To determine TEC function *in vitro*, we established multicellular sTOs consisting of isogenic hPSC-derived TEPs, HPCs, and splanchnic mesenchyme (SM) (Figures 2A and S2A–S2C) (Han et al., 2020; Motazedian et al., 2020). In some cases, expanded 1^o human TM was used in place of hPSC-derived SM. Interestingly, the addition of either primary 1^o TM or hPSC-derived TM resulted in a trend toward higher expression of functional TEC genes, with no significant difference in gene expression between 1^o or iPSC-derived TM (Figure S2D). Immunofluorescence (IF) analysis of sTOs showed KRT5⁺ mTEC-like cells and EPCAM/CD205 DP cells, indicative of TEP-to-TEC development in sTOs (Figures 2B and 2C). We assessed TEC marker expression in TEPs and CD45⁻ sTO cells by qPCR analysis. While *FOXP1* and *KRT8* expression did not differ significantly, *KRT5*, *DLL4*, and *HLA-DR* expression were significantly higher in sTOs (Figure 2D). Cytometry by time of flight (CyTOF) and FC analysis confirmed protein expression of EPCAM, KRT8, HLA-DR, and CD205 in sTOs (Figures 2E–2G). Utilizing the *FOXP1-GFP* hESC reporter line, we quantified FOXP1 expression in sTOs and found that GFP expression is maintained in sTOs (Figure 2H). Taken together, sTOs provide a convenient model system for human TEP/TEC

(C–H) FC plots and quantification of EPCAM/HLA-DR (C and D), EPCAM/CD205 (E and F), and EPCAM/GFP (G and H) expression in day 16–22 TEPs and week 2 TEP-only sTOs.

(I) tSNE plots of EPCAM, HLA-DR, CD205, and GFP expression in 16–22 TEPs and week 2 TEP-only sTOs, n = 3 ind. exp., 1 hPSC line. Plots show percentage of the mean; data are shown as mean ± SEM.



(legend on next page)



development that can be exploited for basic and translational research efforts.

sTOs support isogenic, stem cell-derived T cell development

To test if sTOs could support T cell development *in vitro*, we evaluated pro-T and T cell marker expression in sTOs using 1° thymus samples as controls. After 4 weeks, CD45⁺ cells account for ~44% of live cells in sTOs (Figure 3A). Interestingly, the proportion of DN and CD5⁻ pro-T cells is significantly higher in sTOs than in 1° thymus, while the proportion of early thymic progenitors (ETPs; CD45⁺: CD4/CD8 DN: CD5⁻/CD7⁻) is significantly lower (Figures 3A and 3B) (Awong et al., 2013). CD4/CD8 DP developing thymocytes make up ~17% of CD45⁺ cells, similar to 1° thymocytes (Figures 3A and 3B). ~64% of CD45⁺ cells co-express T cell markers CD3 and T cell receptor (TCR) α/β , indicating positive selection and TCR rearrangement in sTOs (Figures 3C and 3D). While the proportion of CD4/CD8 DP cells does not differ significantly, the proportion of CD4 single positive (SP) cells is significantly higher in 1° thymi, while the proportions of CD8 SP and DN cells are significantly higher in sTOs (Figures 3C and 3D).

We performed CyTOF analysis to further interrogate thymocyte development in week 4 sTOs. cKIT (CD117), a pre-thymocyte commitment marker, was prominently expressed by sTO CD45⁺ cells, with a subset of CD117⁺ cells expressing the early thymocyte transcription factor TCF1 (Figures 3E and 3F). Terminal deoxynucleotidyl transferase (TdT) was detected in both sTO and thymus samples, further confirming TCR rearrangement in sTOs (Figures 3G–3I). Gamma delta ($\gamma\delta$) T cells, invariant natural killer T (iNKT) cells, and NK cells also develop in the thymus (Hogquist and Georgiev, 2020; Ribeiro et al., 2010; Takaba and Takayanagi, 2017). We detected CD3⁺/TCR $\gamma\delta$ ⁺ T cells, CD3⁺/CD56⁺ iNKT cells, and CD3⁻/CD56⁺ NK cells in sTOs (Figures S3A–S3D). To determine if sTO-derived T cells were functional, we cultured dissociated sTOs and human peripheral blood mononuclear cells (PBMCs) with anti-CD3/CD28 Dynabeads and observed a significant increase in the proportion of CD4⁺ and CD4⁺/CD25⁺ cells in stimulated sTOs, albeit at lower levels than observed in PBMC controls (Figures 3J, 3K, S3E, and S3F).

Together, these data demonstrate that sTOs can support functional thymocyte development *in vitro*, as demonstrated by the expression of canonical developmental markers and *in vitro* T cell stimulation. Additionally, sTOs support $\gamma\delta$ T cell, iNKT cell, and NK cell development. Thus, sTOs provide an innovative *in vitro* model to interrogate T cell development in an isogenic, patient-specific manner.

sTOs contain AIRE⁺ mTECs and Tregs

AIRE expression by mTECs mediates negative selection of autoreactive thymocytes (Anderson et al., 2002). Indeed, AIRE⁺ cells are present in sTOs, indicating mTEC development in sTOs (Figure 4A). By IF and FC, we detected CD3⁺/PD-1⁺ cells in sTOs, indicative of ongoing negative selection (Figures 4B–4D) (Baldwin and Hogquist, 2007). To determine if sTOs could support Treg development, we evaluated FOXP3 expression in CD4⁺/CD25⁺ cells by FC and confirmed *FOXP3* expression in sTOs by qPCR (Figures 4E–4G). Furthermore, TRA transcripts are detected in CD45⁻ sTO cells, further corroborating this finding (Figure 4H). These data indicate the occurrence of negative selection in sTOs *in vitro*, albeit at low levels, and provide a basis for further work and optimization.

DISCUSSION

Here, we describe the generation of functional patient-specific sTOs that support hPSC-derived TEC and T cell development *in vitro*. We anticipate that our work provides important conceptual and technical advances for the field and establishes the basis for the development of cell therapy approaches for the treatment of thymic insufficiency and other immunological disorders.

We optimized our hPSC-to-TEP differentiation protocol and demonstrate a role for activin A and BMP4 inhibition in the generation of TEPs *in vitro*, confirming previous mouse studies and illustrating the utility of *in vitro* differentiation in elucidating signaling pathways involved in human TEP/TEC development (Lepletier et al., 2019; Ramos et al., 2021). This platform could be further leveraged to elucidate additional factors necessary for human thymus development, function, and homeostasis; to enhance TEP differentiation for cell replacement therapies; and to

Figure 2. sTOs support TEC development

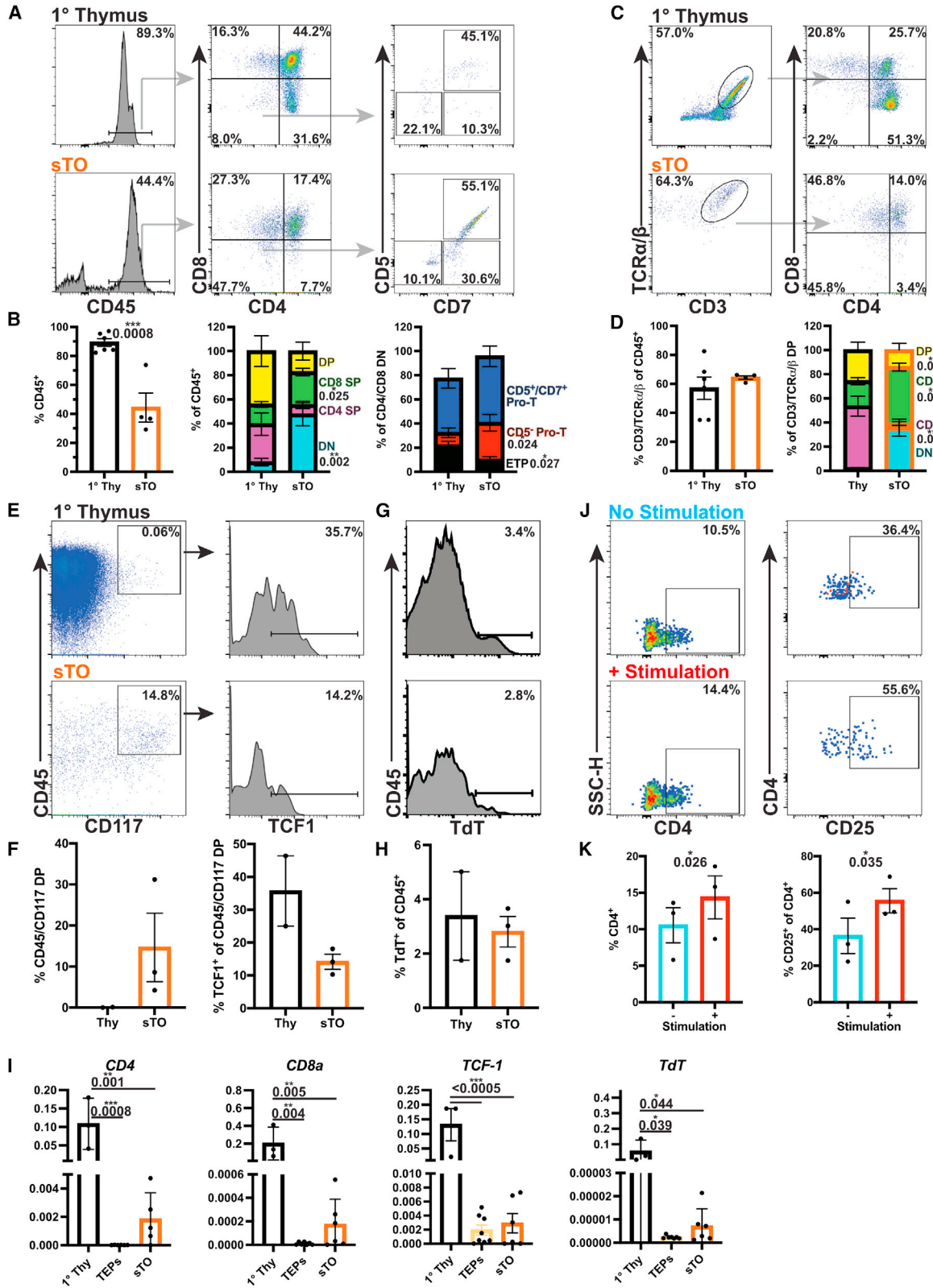
(A) Schematic of multicellular, isogenic sTOs.

(B and C) Representative IF images of KRT8 and KRT5 (B) or EPCAM and CD205 (C) in 1° thymus and sTOs (thymi, n = 3; sTOs, n = 9 ind. exp., 2 hPSC lines).

(D) qPCR analysis of TEC markers in day 17–30 TEPs and week 4 CD45⁻ sTO cells (thymi, n = 3; TEPs, n = 7 ind. exp., 2 hPSC lines; sTOs, n = 4 ind. exp., 2 hPSC lines). p values were determined by t test.

(E–H) CyTOF (E) and FC (F–H) plots and quantification of TEC markers in 1° thymus and sTOs (CyTOF: thymi, n = 2; sTOs, n = 3–6 ind. exp., 3 hPSC lines; FC: thymi, n = 4, sTOs, n = 4–6 ind. exp., 2 hPSC lines).

Plots show percentage of the mean; data are shown as mean \pm SEM.



(legend on next page)



identify novel targets to treat thymic disorders and promote thymic regeneration.

1° TEC cultures require direct air exposure to remain functional (Ceredig et al., 1989; Han and Zúñiga-Pflücker, 2021; Watanabe and Katsura, 1993; Watson et al., 1989). Attempts to culture sTOs as submerged hanging-drop cultures produced CD3⁻/TCR $\alpha\beta$ ⁺ thymocytes stalled at the CD4/CD8 DP stage (data not shown). This aligns with previous reports of aberrant T cell development *in vitro* in the absence of OP9-DLL4 stromal cells (Motazedian et al., 2020). Indeed, the requirement for high oxygen levels for FOXP1-mediated TEC function was recently reported (Han and Zúñiga-Pflücker, 2021). Thus, direct air exposure, as conferred by air-liquid interface culturing, is required for functional sTOs.

Thymocyte-independent development of KRT5⁺ mTECs has been demonstrated in rodent models with blocks in early T cell development. However, those studies did not account for the presence of other immune cell types that could have provided developmental signals attributed to thymic seeding progenitors and developing thymocytes (Jenkinson et al., 2005; Klug et al., 2002). Here, we demonstrate human TEP-to-TEC development in a system devoid of all immune cells. These findings demonstrate the utility of sTOs to interrogate previously inaccessible aspects of human TEC development.

TM provides factors necessary for TEC development and function, expresses HLA class II molecules, and participates in T cell development (Anderson et al., 1993; Itoi et al., 2007; Jenkinson et al., 2003, 2007). Indeed, integrating mesenchyme in hPSC and 1° cell-derived organoids can improve organoid function (Campinoti et al., 2020; Eicher et al., 2022). While mesenchyme spontaneously develops in sTOs, the addition of mesenchyme results in an increased expression of functional thymic genes, indicating a beneficial role in sTO cultures.

We show that hPSC-derived TEPs can develop to functional TECs and express functional TEC markers when cultured as sTOs. While *FOXP1* expression does not vary significantly between TEPs and sTO CD45⁻ cells, *KRT5*, *DLL4*, and *HLA-DR* expression increases significantly. As sTOs were sorted based on CD45 expression, we preclude the possibility that detected *HLA-DR* transcripts were from HLA-DR⁺/CD45⁺ antigen-presenting cells. IF and

CyTOF analyses confirmed HLA-DR protein expression on EPCAM⁺ cells. CD205 marks TEPs and cTECs and has been used by us as a marker for hPSC-derived TEPs (Campinoti et al., 2020; Ramos et al., 2021). We find EPCAM⁺/CD205⁺ TECs in sTOs by IF analysis, as seen in 1° thymi. Thus, we have established culture conditions amenable for hPSC-derived TEC development *in vitro*.

The thymus facilitates functional T cell development from HPCs. Here, we show that sTOs support T cell development from hPSC-derived HPCs *in vitro*, albeit with reduced cell numbers compared with primary tissue. sTOs contain significantly fewer CD45⁺ and ETP cells but have a higher proportion of DN and CD5⁻ pro-T cells than 1° thymi, indicating delayed developmental kinetics in sTOs. Additionally, we observed significantly fewer CD4 SP and increased CD8 SP T cells in sTOs than in 1° thymi, likely due to reduced HLA class II expression in sTOs. Similarly, MS5-DLL1/4-based ATOs also lack MHC class II expression and fail to generate appreciable numbers of CD4⁺ T cells (Montel-Hagen et al., 2019; Seet et al., 2017). CyTOF analysis of sTOs further confirms thymocyte development in sTOs, as demonstrated by CD117, TCF1, and TDT expression. Importantly, sTO-derived T cells respond to *in vitro* stimulation and upregulate the known activation marker CD25, demonstrating functionality. Thus, sTO-derived TECs support the development of T cells that express canonical markers of T cell development and can respond to stimulation.

Another key function of the thymus is the negative selection of potentially autoreactive T cells, effectuated by AIRE-mediated expression of TRAs. Indeed, we detect AIRE protein and TRA transcripts in sTOs. Congruently, we detect CD3⁺/PD-1⁺ T cells in sTOs, indicative of ongoing negative selection, and CD25⁺/CD4⁺/FOXP3⁺ Tregs in sTOs by FC and qPCR analysis; however, the levels detected in sTOs are lower than observed in primary thymus.

We present a functional multicellular, isogenic sTO system that offers advantages over current thymic organoid models. sTOs eliminate the need for 1° tissue and mouse cell lines, allowing for patient-specific thymic organoids capable of negative selection. We anticipate ongoing optimization of HPC generation from hPSCs will further enhance the utility of the sTOs in the future. Thus, we have established the framework for further basic science and translational

Figure 3. sTOs support isogenic T cell development

(A–D) FC plots (A and C) and quantification (B and D) of thymocytes in 1° thymus and week 4 sTOs.

(E–H) CyTOF plots (E and G) and quantification (F and H) of thymocyte markers in 1° thymus and week 4 sTOs (thymi, n = 6; sTOs, n = 4, 2 hPSC lines).

(I) qPCR analysis of CD4, CD8, and TdT in 1° thymus, TEPs, and sTOs (thymi, n = 3; TEPs, n = 6–7, 4 hPSC lines; sTOs, n = 5–6, 4 hPSC lines). (J and K) FC plots (J) and quantification (K) of CD4 and CD25 expression on stimulated T cells from week 4 sTOs (n = 3 ind. exp., 1 hPSC line).

Plots show percentage of the mean; data are shown as mean \pm SEM; p values were determined by t test.

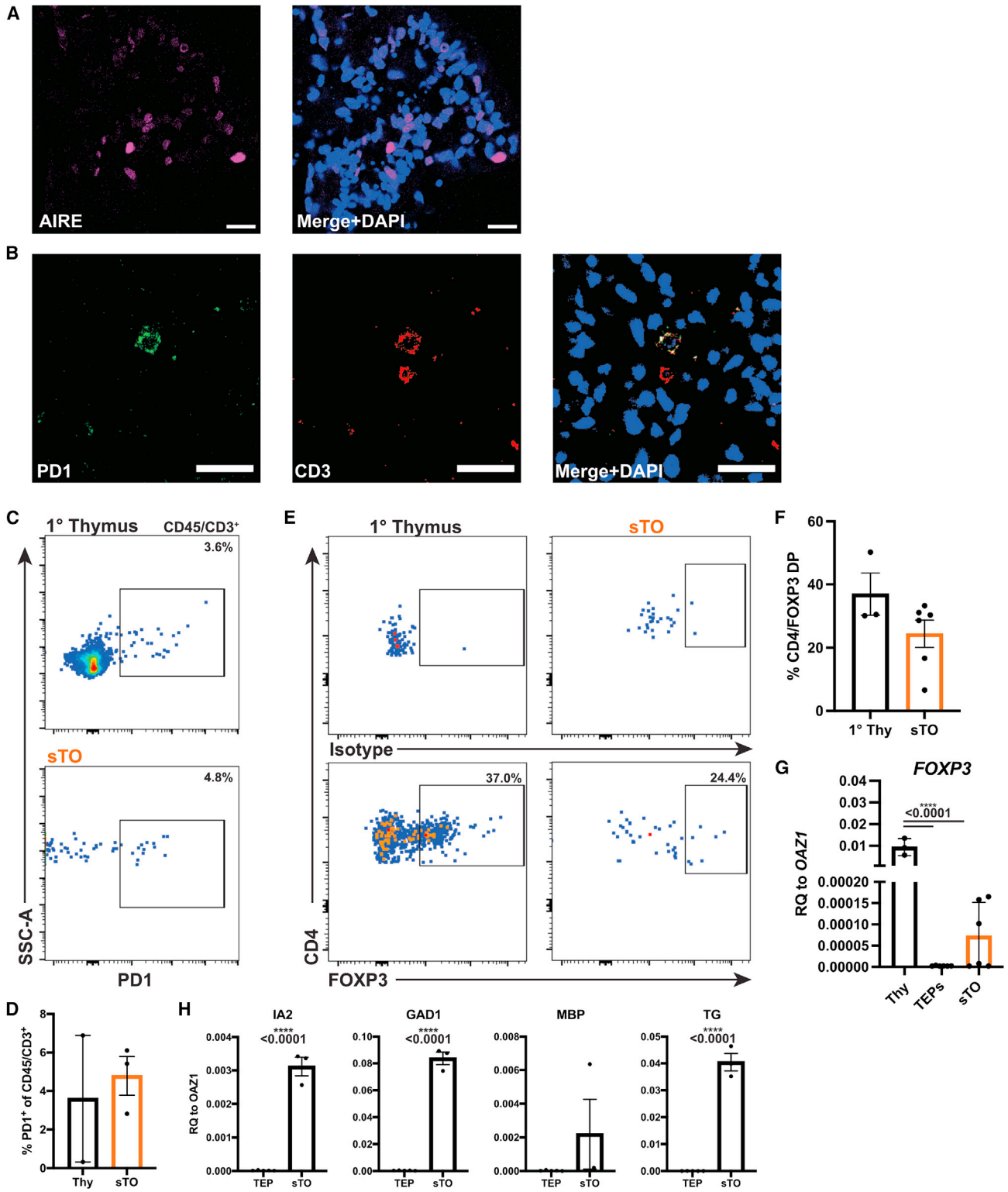


Figure 4. Potential negative selection and Treg development in sTOs

(A) Representative IF image of AIRE in week 4 sTOs (n = 2).

(B) Representative IF image of PD-1 and CD3 in week 4 sTOs (n = 2).

(legend continued on next page)



research interrogating human thymus development and function *in vitro* and in a patient-specific manner.

EXPERIMENTAL PROCEDURES

Resource availability

Corresponding author

Further information and requests for resources and reagents should be directed to and will be fulfilled by the corresponding author, Holger A. Russ (holger.russ@ufl.edu).

Materials availability

All unique/stable reagents generated in this study are available from the corresponding author with a completed materials transfer agreement.

Data and code availability

All data and code generated in this study are available from the corresponding author upon request.

hPSC-to-TEP differentiation

INS-GFP (Micallef et al., 2012) and FOXN1-GFP (Soh et al., 2014) lines, MEL1 hESC lines, or iPSC lines CB2, CB3, CUHM008, and CUHM009 (Ramos et al., 2021) reprogrammed inhouse from PBMCs were cultured on Matrigel (Corning)-coated plates in mTeSR+ (StemCell Technologies). hPSCs were differentiated to TEPs as described (Jenkinson et al., 2005), with some modifications. hPSCs were harvested with TrypLE (Gibco) and resuspended at 10e6 cells/mL in mTeSR+ with 10 μ M Rock inhibitor and seeded at 3.15e5 hPSC/cm² in Matrigel-coated plates in mTeSR+ with 10 μ M Rock inhibitor. 24 h later, cells were washed with koDMEM/F12, and d0 media were added (Table S1). Differentiations were done in X-VIVO10 (Lonza) with added factors (Table S1).

hPSC-to-splanchnic mesoderm differentiation

hPSCs were differentiated to splanchnic mesoderm as previously described (Han et al., 2020). hPSCs were dissociated and plated as described above. 24 h later, cells were washed with koDMEM/F12, and d0 media were added (Table S2). Differentiations were done in Advanced DMEM/F12, N21 (R&D), 15 mM HEPES (Thermo Fisher Scientific), 1 \times Glutamax (Thermo Fisher Scientific), and 1 \times penicillin-streptomycin (Thermo Fisher Scientific) with added factors (Table S2).

hPSC-to-HPC differentiation

hPSCs were differentiated to HPCs as previously described (Motazedian et al., 2020). hPSCs were dissociated, seeded in 6-well suspension plates at 1e6 cells/mL in 5.5 mL Stage I media, and cultured on an orbital shaker rotating at 100 RPM (Table S3). Differ-

entiation continued in suspension through day 7. Day 8 clusters were plated on vitronectin-coated (StemCell Technologies) 0.4 μ m Millicell Transwell inserts (EMD Millipore) at the air-liquid interface and cultured in Stage V media until day 12–20, changing media every other day.

sTO generation

Differentiated cultures at day 18–25 TEPs were mechanically dissociated into small clumps and either combined with 1 $^{\circ}$ (allogenic) TM or day 4–5 splanchnic mesoderm (isogenic) and day 8–20 HPCs at a 1:1:20 mesenchyme:HPC:TEP ratio in a 1.5 mL tube. Cells were pelleted in a swinging-bucket centrifuge at 1,200 RPM for 3 min and resuspended in 5 μ L/sTO Stage V media (Table S3) (Motazedian et al., 2020). A 5 μ L drop was placed on a 0.4 μ m Millicell Transwell insert with 2–3 sTOs per membrane \sim 1 cm apart. Transwells were placed in 6-well plates containing 1.5 mL Stage V media, and media were changed every 2–3 days. sTOs were harvested at indicated times for analysis. For IF analysis, sTOs were fixed on the membranes in 4% PFA for 15–60 min at room temperature (in some cases, sTOs were fixed overnight [ON] at 4 $^{\circ}$ C). After fixation, sTOs were washed 3 \times with PBS and incubated in 30% sucrose at 4 $^{\circ}$ C ON. sTOs were cut from the membrane, embedded in optimal cutting temperature (OCT) medium, and snap frozen. For qPCR analysis, sTOs were harvested from the membrane with 0.5 mL digestion buffer containing 2% FBS, 100 ng/mL DNaseI, 96 μ g/mL Liberase, 0.88 mg/mL Collagenase/Dispase, and 1.25 mg/mL Collagenase D in DMEM and transferred to a 1.5 mL tube. Cells were incubated at 37 $^{\circ}$ C for 6 min and then triturated (3–5 cycles) until sTOs were dissociated. Cells were pelleted using a tabletop centrifuge and resuspended in magnetic-activated cell sorting (MACS) buffer. Cells were incubated with anti-CD45 magnetic beads (Miltenyi) and sorted per manufacturer instructions. Sorted cells were resuspended in Qiagen RLT or QIAzol lysis buffer and used for RNA isolation using RNeasy kits or QIAzol/phenol chloroform (QIAGEN) per manufacturer instructions. For FC analysis, sTOs were digested as described. Cell suspensions were spun down on a tabletop centrifuge, resuspended in 1 mL fluorescence-activated cell sorting (FACS) buffer, and passed through a 40 μ m filter into a 5 mL round-bottom polystyrene FACS tube. Cells were FC blocked (BioLegend) for 10 min at room temperature (RT) and incubated in antibody cocktail for 30 min on ice in the dark (Table S4). Cells were washed with 2 mLs FACS buffer, spun down in a swinging-bucket centrifuge at 1,500 RPM for 3 min, resuspended in 0.2 mL FACS buffer with 2.5 ng/mL DAPI, and analyzed on a Cytek Aurora 5-laser cytometer.

1 $^{\circ}$ thymus processing

Deidentified human thymus samples were obtained from pediatric cardiothoracic surgeries. A \sim 1 cm³ section was minced with a

(C and D) FC plots (C) and quantification (D) of PD-1 expression in CD45⁺/CD3⁺ cells in 1 $^{\circ}$ thymi and week 4 sTOs (thymi, n = 2; sTOs, n = 3 ind. exp., 1 hPSC line).

(E and F) FC plots (E) and quantification (F) of FOXP3 expression in CD25⁺/CD4⁺ cells in 1 $^{\circ}$ thymi and sTOs (thymi, n = 3; sTOs, n = 6 ind. exp., 2 hPSC lines).

(G and H) qPCR analysis of *FOXP3* (G) and TRAs (H) in 1 $^{\circ}$ thymus, TEPs, and week 4 CD45⁺ sTO cells (G: thymi, n = 3; TEPs, n = 6–7 ind. exp., 4 hPSC lines; sTOs, n = 5–6 ind. exp., 4 hPSC lines; H: TEPs, n = 5 ind. exp., 1 hPSC line; sTOs, n = 3 ind. exp., 1 hPSC line).

Plots show percentage of the mean; data are shown as mean \pm SEM; p values were determined by t test.



razorblade in cold PBS and transferred to a 50 mL conical tube, washed with PBS, resuspended in 5–10 mL digestion buffer, and dissociated as above. Cells were quenched in 40 mL DMEM+10% FBS and 1:1,000 DNaseI, filtered through a 70 μ m filter, pelleted by centrifugation at 1,500 RPM for 10 min, counted, and sorted as above. To expand TM, minced thymus pieces were plated in 15 cm plates, cultured in DMEM supplemented with 10% FBS, 1 \times Glutamax, and 1 \times penicillin-streptomycin (Pen/Strep) until confluent, and cryopreserved.

CyTOF

Antibodies used in mass cytometry were purchased as rare-earth metal conjugates from Fluidigm or were custom conjugated in-house using MaxPar X8 conjugation kits (Fluidigm) according to manufacturer specification (Table S4). Human thymus tissue and sTOs were dissociated as described, and single-cell suspensions were washed with Cell Staining Buffer (CSB; Fluidigm) and counted. Tantalum-labeled Veri-Cells (BioLegend) were prepared per manufacturer instructions and spiked into each sample as described (Sahaf et al., 2020). Samples were incubated for 5 min with Fc block (BioLegend) and viability reagents (Cell-ID Intercalator-103Rh, Fluidigm) prior to addition of cell surface antibody staining cocktails for 30 min at RT. After washing, individual samples were barcoded utilizing the CyTOF Cell-ID 20-Plex Palladium Barcoding Kit (Fluidigm) per manufacturer instructions and pooled into a single sample. The combined sample was fixed and permeabilized using the FoxP3 transcription buffer kit (ThermoFisher) and stained for 30 min on ice as described (van der Heide et al., 2022). Immediately prior to acquisition, samples were washed with CSB and Cell Acquisition Solution (CAS; Fluidigm) and resuspended in CAS at a concentration of 10⁶ cells/mL with a 1:20 dilution of EQ normalization beads (Fluidigm). Samples were acquired on a Fluidigm Helios mass cytometer using the wide-bore injector configuration at an acquisition speed of <400 cells per second. FCS files were then normalized and concatenated using Fluidigm's CyTOF software (v.6.7.1016) and analyzed with FlowJo v.10.7 (BD Biosciences).

Quantitative real-time PCR

cDNA synthesis was done using iScript cDNA synthesis kit (Bio-Rad). Quantitative real-time PCR was performed on a CFX96 Touch Real-Time PCR Detection System (Bio-Rad) using human specific probes or primers (Table S5). Data were set relative to *OAZ1* and plotted as the mean \pm standard error of the mean (SEM).

IF

10 μ m sections were cut using a cryostat and placed on microscope slides. Slides were washed in PBS at RT for 10 min and blocked/permeabilized in CAS-block (Invitrogen)+0.2% Triton X-100 for 30 min at RT. Slides were stained for 1 h at RT with 1^o antibodies (Table S4) in CAS-block+0.2% Triton X-100. Slides were washed with PBS+0.1% Tween and incubated in secondary antibodies (Alexa Fluor-tagged secondary antibodies [Invitrogen]) diluted 1:1,000 in PBS+0.1% Tween for 40 min at RT. Slides were washed and mounted with Pro-Long Gold with DAPI (Invitrogen). z stack or snap images were taken with a Zeiss LSM 800 microscope. For all

IF images, the scale bars are 20 μ m, and nuclei were counterstained with DAPI.

T cell activation assay

sTOs were dissociated as described above, plated, and stimulated with Human T-Activator CD3/CD28 dynabeads (Thermo Fisher Scientific: 11131D) in 96-well plates for 5 days, collected, and analyzed by FC.

Statistics

Data were analyzed using GraphPad Prism software. t tests or one-way ANOVAs were performed, as indicated in the figure legends.

Regulatory permissions

PBMC collection from human subjects was approved by the Colorado Multiple Institutional Review Board (COMIRB #14-0842; principal investigator: A.J.). Use of deidentified human neonatal thymus tissue was approved by COMIRB (COMIRB #18-0347; principal investigator: H.A.R.).

SUPPLEMENTAL INFORMATION

Supplemental information can be found online at <https://doi.org/10.1016/j.stemcr.2023.02.013>.

AUTHOR CONTRIBUTIONS

S.A.R., L.H.A., J.J.M., D.H., G.K., N.A., and D.H. conducted the experiments. S.A.R., L.H.A., J.J.M., D.H., A.J., and H.A.R. designed the experiments. A.J. and H.A.R. supervised the study. S.A.R. and H.A.R. wrote the manuscript, and all authors reviewed, edited, and agreed on its contents.

ACKNOWLEDGMENTS

We acknowledge the organ donors and their families and Dr. James Jagers, MD (Children's Colorado Hospital), for providing access to patient samples. The Russ lab is or was supported by NIH/NIDDK grants R01DK12044 and P30DK116073; NIDDK/HIRN RRID: SCR_014393; UC24 DK104162; the Culshaw Junior Investigator Award in Diabetes; the Children's Diabetes Foundation; and the Gate's Grubstake Fund. The Jimeno lab is supported by National Institutes of Health grants R01CA149456, R01CA213102, and P30-CA046934 (University of Colorado Cancer Center Support Grant) and the Daniel and Janet Mordecai Foundation. D.H. is supported by NIH/NIDDK P30DK020541, U01K123716, R01DK130425.

CONFLICT OF INTERESTS

A.J. consults for SuviCa and owns stock options in SuviCa and Champions Oncology. H.A.R. was a SAB member at Sigilon Therapeutics and Prellis Biologics and consulted for Eli Lilly and Minutia. S.A.R., L.H.A., J.J.M., A.J., and H.A.R. filed patent applications based on this work.

Received: June 13, 2022

Revised: February 25, 2023

Accepted: February 26, 2023

Published: March 23, 2023



REFERENCES

- Anderson, G., Jenkinson, E.J., Moore, N.C., and Owen, J.J.T. (1993). MHC class II-positive epithelium and mesenchyme cells are both required for T-cell development in the thymus. *Nature* 362, 70–73. <https://doi.org/10.1038/362070a0>.
- Anderson, M.S., Venanzi, E.S., Klein, L., Chen, Z., Berzins, S.P., Turlay, S.J., von Boehmer, H., Bronson, R., Dierich, A., Benoist, C., and Mathis, D. (2002). Projection of an immunological self shadow within the thymus by the Aire protein. *Science* 298, 1395–1401. <https://doi.org/10.1126/science.1077464>.
- Auerbach, R. (1960). Morphogenetic interactions in the development of the mouse thymus gland. *Dev. Biol.* 2, 271–284.
- Awong, G., Singh, J., Mohtashami, M., Malm, M., La Motte-Mohs, R.N., Benveniste, P.M., Serra, P., Herer, E., Van Den Brink, M.R., and Zúñiga-Pflücker, J.C. (2013). Human proT-cells generated in vitro facilitate hematopoietic stem cell-derived T-lymphopoiesis in vivo and restore thymic architecture. *Blood* 122, 4210–4219. <https://doi.org/10.1182/blood>.
- Baldwin, T.A., and Hogquist, K.A. (2007). Transcriptional analysis of clonal deletion in vivo. *J. Immunol.* 179, 837–844. <https://doi.org/10.4049/jimmunol.179.2.837>.
- Campinoti, S., Gjinovci, A., Ragazzini, R., Zanieri, L., Ariza-McNaughton, L., Catucci, M., Boeing, S., Park, J.-E., Hutchinson, J.C., Muñoz-Ruiz, M., et al. (2020). Reconstitution of a functional human thymus by postnatal stromal progenitor cells and natural whole-organ scaffolds. *Nat. Commun.* 11, 6372. <https://doi.org/10.1038/s41467-020-20082-7>.
- Ceredig, R., Medveczky, J., and Skulimowski, A. (1989). MOUSE FETAL THYMUS LOBES CULTURED IN IL-2 GENERATE CD3+, TCR-gamma/delta-EXPRESSING CD4-/CD8+ AND CD4-/CD8-CELLS. *J. Immunol.* 142, 3353–3360.
- Chhatta, A.R., Cordes, M., Hanegraaf, M.A.J., Vloemans, S., Cupedo, T., Cornelissen, J.J., Carlotti, F., Salvatori, D., Pike-Overzet, K., Fibbe, W.E., et al. (2019). De novo generation of a functional human thymus from induced pluripotent stem cells. *J. Allergy Clin. Immunol.* 144, 1416–1419.e7. <https://doi.org/10.1016/j.jaci.2019.09.013>.
- Chung, B., Montel-Hagen, A., Ge, S., Blumberg, G., Kim, K., Klein, S., Zhu, Y., Parekh, C., Balamurugan, A., Yang, O.O., and Crooks, G.M. (2014). Engineering the human thymic microenvironment to support thymopoiesis in vivo. *Stem Cell.* 32, 2386–2396. <https://doi.org/10.1002/stem.1731>.
- Coder, B.D., Wang, H., Ruan, L., and Su, D.-M. (2015). Thymic involution perturbs negative selection leading to autoreactive T cells that induce chronic inflammation. *J. Immunol.* 194, 5825–5837. <https://doi.org/10.4049/jimmunol.1500082>.
- Duah, M., Li, L., Shen, J., Lan, Q., Pan, B., and Xu, K. (2021). Thymus degeneration and regeneration. *Front. Immunol.* 12 (ptember), 706244. <https://doi.org/10.3389/fimmu.2021.706244>.
- Eicher, A.K., Kechele, D.O., Sundaram, N., Berns, H.M., Poling, H.M., Haines, L.E., Sanchez, J.G., Kishimoto, K., Krishnamurthy, M., Han, L., et al. (2022). Functional human gastrointestinal organoids can be engineered from three primary germ layers derived separately from pluripotent stem cells. *Cell Stem Cell* 29, 36–51.e6. <https://doi.org/10.1016/j.stem.2021.10.010>.
- Han, J., and Zúñiga-Pflücker, J.C. (2021). High-oxygen submersion fetal thymus organ cultures enable FOXP1-dependent and -independent support of T lymphopoiesis. *Front. Immunol.* 12, 652665. <https://doi.org/10.3389/fimmu.2021.652665>.
- Han, L., Chaturvedi, P., Kishimoto, K., Koike, H., Nasr, T., Iwasawa, K., Giesbrecht, K., Witcher, P.C., Eicher, A., Haines, L., et al. (2020). Single cell transcriptomics identifies a signaling network coordinating endoderm and mesoderm diversification during foregut organogenesis. *Nat. Commun.* 11, 4158. <https://doi.org/10.1038/s41467-020-17968-x>.
- Hogquist, K., and Georgiev, H. (2020). Recent advances in iNKT cell development [version 1; peer review: 3 approved]. *F1000Res.* 9, F1000.Faculty Rev-127. <https://doi.org/10.12688/f1000research.21378.1>.
- Itoi, M., Tsukamoto, N., Yoshida, H., and Amagai, T. (2007). Mesenchymal cells are required for functional development of thymic epithelial cells. *Int. Immunol.* 19, 953–964. <https://doi.org/10.1093/intimm/dxm060>.
- Janda, A., Sedlacek, P., Hönig, M., Friedrich, W., Champagne, M., Matsumoto, T., Fischer, A., Neven, B., Contet, A., Bensoussan, D., et al. (2010). Multicenter survey on the outcome of transplantation of hematopoietic cells in patients with the complete form of Di-George anomaly. *Blood* 116, 2229–2236.
- Jenkinson, W.E., Jenkinson, E.J., and Anderson, G. (2003). Differential requirement for mesenchyme in the proliferation and maturation of thymic epithelial progenitors. *J. Exp. Med.* 198, 325–332. <https://doi.org/10.1084/jem.20022135>.
- Jenkinson, W.E., Rossi, S.W., Jenkinson, E.J., and Anderson, G. (2005). Development of functional thymic epithelial cells occurs independently of lymphostromal interactions. *Mech. Dev.* 122, 1294–1299. <https://doi.org/10.1016/j.mod.2005.08.003>.
- Jenkinson, W.E., Rossi, S.W., Parnell, S.M., Jenkinson, E.J., and Anderson, G. (2007). PDGFR-expressing mesenchyme regulates thymus growth and the availability of intrathymic niches. *Blood* 109, 954–960. <https://doi.org/10.1182/blood-2006>.
- Kadouri, N., Nevo, S., Goldfarb, Y., and Abramson, J. (2020). Thymic epithelial cell heterogeneity: TEC by TEC. *Nat. Rev. Immunol.* 20, 239–253. <https://doi.org/10.1038/s41577-019-0238-0>.
- Klug, D.B., Carter, C., Gimenez-Conti, I.B., and Richie, E.R. (2002). Cutting edge: thymocyte-independent and thymocyte-dependent phases of epithelial patterning in the fetal thymus. *J. Immunol.* 169, 2842–2845. <https://doi.org/10.4049/jimmunol.169.6.2842>.
- Kreins, A.Y., Bonfanti, P., and Davies, E.G. (2021). Current and future therapeutic approaches for thymic stromal cell defects. *Front. Immunol.* 12, 655354. <https://doi.org/10.3389/fimmu.2021.655354>.
- Lepletier, A., Hun, M.L., Hammett, M.V., Wong, K., Naeem, H., Hedger, M., Loveland, K., and Chidgey, A.P. (2019). Interplay between follistatin, Activin A, and BMP4 signaling regulates postnatal thymic epithelial progenitor cell differentiation during aging. *Cell Rep.* 27, 3887–3901.e4. <https://doi.org/10.1016/j.celrep.2019.05.045>.
- Mandel, T.E., and Kennedy, M.M. (1978). The differentiation of murine thymocytes in vivo and in vitro. *Immunology* 35, 317–331.
- Micallef, S.J., Li, X., Schiesser, J.V., Hirst, C.E., Yu, Q.C., Lim, S.M., Nostro, M.C., Elliott, D.A., Sarangi, F., Harrison, L.C., et al. (2012).



- INS GFP/w human embryonic stem cells facilitate isolation of in vitro derived insulin-producing cells. *Diabetologia* 55, 694–706. <https://doi.org/10.1007/s00125-011-2379-y>.
- Montel-Hagen, A., Seet, C.S., Li, S., Chick, B., Zhu, Y., Chang, P., Tsai, S., Sun, V., Lopez, S., Chen, H.-C., et al. (2019). Organoid-induced differentiation of conventional T cells from human pluripotent stem cells. *Cell Stem Cell* 24, 376–389.e8. <https://doi.org/10.1016/j.stem.2018.12.011>.
- Motazedian, A., Bruveris, F.E., Kumar, S.V., Schiesser, J.V., Chen, T., Ng, E.S., Chidgey, A.P., Wells, C.A., Elefanty, A.G., and Stanley, E.G. (2020). Multipotent RAG1+ progenitors emerge directly from haemogenic endothelium in human pluripotent stem cell-derived haematopoietic organoids. *Nat. Cell Biol.* 22, 60–73. <https://doi.org/10.1038/s41556-019-0445-8>.
- Palmer, D.B. (2013). The effect of age on thymic function. *Front. Immunol.* 4, 316. <https://doi.org/10.3389/fimmu.2013.00316>.
- Parent, A.V., Russ, H.A., Khan, I.S., Laflam, T.N., Metzger, T.C., Anderson, M.S., and Hebrok, M. (2013). Generation of functional thymic epithelium from human embryonic stem cells that supports host T cell development. *Cell Stem Cell* 13, 219–229. <https://doi.org/10.1016/j.stem.2013.04.004>.
- Ramos, S.A., Morton, J.J., Yadav, P., Reed, B., Alizadeh, S.I., Shilleh, A.H., Perrenoud, L., Jaggers, J., Kappler, J., Jimeno, A., and Russ, H.A. (2021). Generation of functional human thymic cells from induced pluripotent stem cells. *J. Allergy Clin. Immunol.* 149, 767–781.e6. <https://doi.org/10.1016/j.jaci.2021.07.021>.
- Ribeiro, V.S.G., Hasan, M., Wilson, A., Boucontet, L., Pereira, P., Lesjean-Pottier, S., Satoh-Takayama, N., Di Santo, J.P., and Vosshenrich, C.A.J. (2010). Cutting edge: thymic NK cells develop independently from T cell precursors. *J. Immunol.* 185, 4993–4997. <https://doi.org/10.4049/jimmunol.1002273>.
- Sahaf, B., Rahman, A., Maecker, H.T., and Bendall, S.C. (2020). High-parameter immune profiling with CyTOF. *Methods Mol. Biol.* 2055, 351–368. https://doi.org/10.1007/978-1-4939-9773-2_16.
- Seet, C.S., He, C., Bethune, M.T., Li, S., Chick, B., Gschwend, E.H., Zhu, Y., Kim, K., Kohn, D.B., Baltimore, D., et al. (2017). Generation of mature T cells from human hematopoietic stem and progenitor cells in artificial thymic organoids. *Nat. Methods* 14, 521–530. <https://doi.org/10.1038/nmeth.4237>.
- Soh, C.-L., Giudice, A., Jenny, R.A., Elliott, D.A., Hatzistavrou, T., Micallef, S.J., Kianizad, K., Seach, N., Zúñiga-Pflücker, J.C., Chidgey, A.P., et al. (2014). FOXP1 GFP/w reporter hESCs enable identification of integrin-b4, HLA-DR, and EpCAM as markers of human PSC-derived FOXP1 + thymic epithelial progenitors. *Stem Cell Rep.* 2, 925–937. <https://doi.org/10.1016/j.stemcr.2014.04.009>.
- Volpi, S., Yamazaki, Y., Brauer, P.M., van Rooijen, E., Hayashida, A., Slavotinek, A., Sun, K.H., Di Rocco, M., Rivolta, C., Bortolomai, I., et al. (2017). EXTL3 mutations cause skeletal dysplasia, immune deficiency, and developmental delay. *J. Exp. Med.* 214, 623–637. <https://doi.org/10.1084/jem.20161525>.
- Sun, X., Xu, J., Lu, H., Liu, W., Miao, Z., Sui, X., Liu, H., Su, L., Du, W., He, Q., et al. (2013). Directed differentiation of human embryonic stem cells into thymic epithelial progenitor-like cells reconstitutes the thymic microenvironment in vivo. *Cell Stem Cell* 13, 230–236. <https://doi.org/10.1016/j.stem.2013.06.014>.
- Takaba, H., and Takayanagi, H. (2017). The mechanisms of T cell selection in the thymus. *Trends Immunol.* 38, 805–816. <https://doi.org/10.1016/j.it.2017.07.010>.
- Schmitt, T.M., and Zúñiga-Pflücker, J.C. (2002). Induction of T Cell development from hematopoietic progenitor cells by delta-like-1 in vitro. *Immunity* 17, 749–756.
- van der Heide, V., Jangra, S., Cohen, P., Rathnasinghe, R., Aslam, S., Aydilto, T., Geanon, D., Handler, D., Kelley, G., Lee, B., et al. (2022). Limited extent and consequences of pancreatic SARS-CoV-2 infection. *Cell Rep.* 38, 110508. <https://doi.org/10.1016/J.CELREP.2022.110508>.
- Watanabe, Y., and Katsura, Y. (1993). Development of T cell receptor $\alpha\beta$ -bearing T cells in the submersion organ culture of murine fetal thymus at high oxygen concentration. *Eur. J. Immunol.* 23, 200–205. <https://doi.org/10.1002/eji.1830230131>.
- Watson, J.D., Morrissey, P.J., Namen, A.E., Conlon, P.J., and Widmer, M.B. (1989). Effect of IL-7 on the growth of fetal thymocytes in culture. *J. Immunol.* 143, 1215–1222.